Structural Transformations of Oligomeric Intermediates in the Fibrillation of the Immunoglobulin Light Chain LEN†

Pierre O. Souillac, Vladimir N. Uversky, and Anthony L. Fink*

Department of Chemistry and Biochemistry, University of California, Santa Cruz, California 95064

Received April 25, 2003

ABSTRACT: LEN is a κIV immunoglobulin light chain variable domain from a patient suffering from multiple myeloma but with no evidence of amyloid fibrils. However, fibrils are formed when LEN solutions are agitated under mildly destabilizing conditions. Surprisingly, an inverse concentration dependence was observed on the kinetics of fibril formation because of the formation of off-pathway soluble oligomers at high protein concentration. Despite the fact that most of the protein is present in the off-pathway intermediates at relatively early times of aggregation, eventually all the protein forms fibrils. Thus, a structural rearrangement from the non fibril-prone off-pathway oligomers to a more fibril-prone species must occur. A variety of techniques were used to monitor changes in the size, secondary structure, solvent accessibility, and intrinsic stability of the oligomers, as a function of incubation time. The structural rearrangement was accompanied by a significant increase of disordered secondary structure, an increase in solvent accessibility, and a decrease in intrinsic stability of the soluble oligomeric species. We conclude that fibrils arise from the oligomers containing a less stable conformation of LEN, either directly or via dissociation. This is the first fibrillating system in which soluble off-pathway oligomeric intermediates have been shown to be the major transient species and in which fibrillation occurs from a relatively unfolded conformation present in these intermediates.

Amyloidoses result from the deposition of normally soluble proteins leading to impairment of various organ functions. Partially folded intermediates of such proteins have been shown to be responsible for the initiation of the association process leading to the irreversible formation of these insoluble fibrils (*1*−*4*). Light chain amyloidosis (AL or primary amyloidosis) originates from the formation and systemic deposition (especially in the kidneys) of fibrils of monoclonal immunoglobulin light chain variable domains in patients suffering from multiple myeloma (*5*−*7*). LEN, originally isolated from the urine of a patient with multiple myeloma, is the variable domain of an immunoglobulin light chain (κIV Bence Jones protein). Despite the lack of in vivo evidence of amyloidosis (*8*), LEN fibrils were readily observed in vitro upon vigorous stirring under mildly destabilizing conditions (pH 2 or pH 7 with low amounts of urea) and physiological pH. Surprisingly, at both pH 2 and 7, inverse concentration dependencies were observed on the kinetics of fibril formation; the kinetics becoming slower with increasing protein concentrations (*9*, *10*). At both pHs, inverse linear relationships between the amount of dimers initially present in solution and the time necessary to form fibrils were observed, indicating the critical role of the dimer/monomer equilibrium on fibril formation. In fact, variable domains have a tendency to form relatively tight dimers with dissociation constants between 1 μM and 1 mM (*11*). Under native conditions (pH 7), the self-dissociation constant of LEN was determined to be 10 μM (*7*), and 62 μM at pH 2 (*9*), reflecting a small destabilization of the dimers upon lowering the pH. At pH 7, the fibrils were formed directly, with no nonfibrillar association being detected. This observation, and the inverse concentration dependence, suggests that dissociation of the dimers was the limiting step of the reaction. On the other hand, at pH 2, despite the nativelike character of LEN, the immediate formation of off-pathway soluble oligomers was observed at high protein concentration (where significant amounts of nativelike dimers were present), suggesting that the off-pathway species were responsible for the delayed formation of fibrils (*9*). However, despite the off-pathway trapping of most of the protein, fibrils were still formed (with transition midpoints close to 50 h). Interestingly, no precipitates were observed during the off-pathway formation phase, cloudiness appearing only upon fibril formation or after about 24 h. At low protein concentration (where few dimers were initially present), fibrils were formed directly (i.e., no off-pathway association was observed) with significantly faster kinetics (transition midpoints close to 5 h) (*9*). These observations suggest that these off-pathway species were probably formed from nonspecific oligomerization of destabilized dimers. Furthermore, electron microscopy images clearly showed that, even at high protein concentration, only fibrils were present at the end of the reaction, no amorphous aggregates being observed (*9*). In addition, all material was pelletable by the end of the reaction, reflecting the fact that no protein was left as soluble off-pathway oligomers. These two observations indicated the

† This research was supported by a grant from the National Institutes of Health (DK55675).

* Corresponding author. Tel: (831) 459-2744. Fax: (831) 459-2744. E-mail: enzyme@cats.ucsc.edu.

10.1021/bi034652m CCC: $25.00
Published on Web 06/13/2003

reversibility of the nonspecific initial association and the fact that a structural rearrangement step, leading to the formation of fibril-prone species, had to occur.

The purpose of this study was to investigate the structural reorganization step in which the off-pathway soluble oligomers were converted to fibril-prone species, under conditions were most protein was initially trapped as the off-pathway species. Static light scattering, fluorescence anisotropy, far-UV circular dichroism (CD), attenuated total reflectance Fourier transform infrared (ATR-FTIR), H/D exchange, acrylamide quenching, urea stability, and pepsin proteolysis were used to monitor changes occurring to the species in solution as a function of incubation time.

MATERIALS AND METHODS

Chemicals. Ultrapure urea was purchased from ICN Biomedicals, Aurora, OH. Peptone and yeast extract used in the medium were purchased from Difco, MD. All other chemicals were purchased from Fisher Scientific, NJ and were of the highest grade available. The water used throughout the study was doubly deionized.

LEN Purification. Escherichia coli JM83 cloned with the plasmid pkIVlen004, expression system generously given by Dr. F. Stevens (*7*), was grown in a rich medium containing carbenicillin (75 μg/mL). Sucrose and water extracts were pooled together, dialyzed against a 10 mM Tris buffer at pH 8.0, and eluted through a mono-Q column (BioRad, Hercules, CA). After dialysis against a 10 mM acetate buffer at pH 4.0, the flow through from the mono-Q column was loaded onto a mono-S column (Pharmacia, Mississuaga, Canada). LEN was eluted using a NaCl gradient from 0 to 120 mM over 20 min. The purest fractions were pooled, dialyzed against 10 mM phosphate buffer solution at pH 8.0, and concentrated by ultrafiltration to about 4 mg/mL. LEN purity was assessed by SDS gel electrophoresis and mass spectroscopy.

In Vitro Off-Pathway Oligomer and Fibril Formation Procedure. In vitro fibril formation was studied by incubating solutions of LEN at pH 2 (20 mM HCl and 100 mM NaCl) and 3 mg/mL (240 μM) at 37 °C with stirring. The solutions, with volumes ranging from 200 to 400 μL, were stirred in 2 mL HPLC glass vials (Fisher, Pittsburgh, PA) containing microstirrer bars (8 × 1.5 mm; Fisher). The stirring rate was ca. 660 rpm. Aliquots of different volumes (depending on the analytical method used) were withdrawn at predetermined time points during the kinetics, further diluted, and tested using various biophysical techniques. Depending on the time of stirring, off-pathway oligomers and/or fibrils were present in the samples.

Thioflavin T and ANS Fluorescence. Fluorescence measurements were performed using a FluoroMax-2 fluorescence spectrophotometer (Jobin Yvon-Spex, Edison, NJ). All measurements were performed at 37 °C with final protein concentrations of 0.015 mg/mL. ANS fluorescence measurements were performed using an excitation wavelength of 380 nm and recording the emission spectra from 420 to 600 nm. Thioflavin T (ThT) fluorescence measurements were performed using an excitation wavelength of 450 nm and recording the emission spectra from 465 to 560 nm. Solutions of 10 μM ANS or ThT at pH 2 (20 mM HCl and 100 mM NaCl) were used throughout the study. The various fluorescence measurements (intensity and λ_{max}) were plotted versus time and fitted by a sigmoidal curve allowing slope variations of the initial and final phases (*12*).

Transmission Electron Microscopy. The formation of fibrils on stirring 3.0 mg/mL LEN solutions at 37 °C was assessed by EM. After a 2-fold dilution of the aliquots, 5 mL of protein samples was placed on Formavar-coated copper grids. After draining the excess sample with filter paper, the grids were air-dried. A freshly prepared 2% (w/v) uranyl acetate solution was then applied on the grids. After removal of the excess negative staining solution, the grids were air-dried again. Electron micrographs were collected using a JEOL JEM-100B microscope with a voltage accelerator of 80 kV. A magnification of 50 000 was used.

Steady-State Fluorescence Anisotropy. Changes in fluorescence anisotropy on stirring LEN solutions at pH 2 and 3 mg/mL were measured using a FluoroMax-3 fluorescence spectrophotometer (Jobin Yvon-Spex). LEN solutions of 3 mg/mL (240 mM) at pH 2 (20 mM HCl and 100 mM NaCl) were stirred at 37 °C and 660 rpm in a 2 mL HPLC glass vial containing a microstirrer bar. Aliquots of 5 μL of the protein solution were withdrawn at predetermined time points and diluted into 995 μL of a pH 2 dilution solution (20 mM HCl and 100 mM NaCl) to obtain a final protein concentration of 0.01 mg/mL. The wavelengths of excitation and emission were set at 280 nm (with a slit opening of 5 nm) and 350 nm (with a slit opening of 5 nm), respectively. The instrumental correction factor was determined before each anisotropy measurement by taking, under the same experimental conditions, the ratio of the fluorescence intensity with the excitation polarizer in the horizontal position and the emission polarizer in the vertical position (I_{HV}) with that measured with the excitation polarizer in the horizontal position and the emission polarizer in the horizontal position (I_{HH}):

$$G_{(\lambda EM)} = \frac{I_{HV}}{I_{HH}} \quad (1)$$

Steady-state anisotropies were calculated from the fluorescence intensities obtained with the excitation polarizer in the vertical position and the emission polarizer in either the vertical (I_{VV}) or the horizontal position (I_{VH}) and the *G*-factor previously determined using the following equation:

$$r = \frac{I_{VV} - GI_{VH}}{I_{VV} + 2GI_{VH}} \quad (2)$$

The measurements were performed in triplicate.

Thin Film Attenuated Total Reflectance Fourier Transform Infrared Spectroscopy (ATR-FTIR). FTIR spectra of LEN solution at pH 2 (20 mM HCl and 100 mM NaCl) were recorded as a function of stirring time using a ThermoNicolet Nexus 670 FTIR spectrophotometer from 4000 to 400 cm^{-1} using a 4 cm^{-1} resolution and an accumulation of 512 scans. Protein solutions at pH 2 and 3 mg/mL (240 μM) were stirred at 37 °C and 630 rpm in a 2 mL HPLC glass vial containing a microstirrer bar. Aliquots of 40 μL were withdrawn after 0, 4, 12, and 80 h of stirring. These aliquots were evenly dried on the surface of a germanium crystal using nitrogen to form a hydrated thin film. The system was continuously purged with dry nitrogen. Background and water vapor

subtractions were performed until a straight baseline was obtained between 2000 and 1750 cm^{-1}. Curve fitting of the amide I regions (raw spectra) was performed using mixed Gaussian/Lorentzian functions (Galactic PeakSolve, Version 1.05, Galactic Industries). Second derivative and Fourier self-deconvoluted spectra were used as a peak position guide for the curve fitting procedure.

H/D Exchange. The rates and extents of hydrogen/deuterium exchange of LEN solution at pH 2 (20 mM HCl and 100 mM NaCl) were measured as a function of stirring time. Protein solutions of 3 mg/mL were stirred at 37 °C and 630 rpm in a 2 mL HPLC glass vial containing a microstirrer bar. Aliquots of 40 μL were withdrawn after 0, 4, 12, and 80 h of stirring. These aliquots were evenly dried with nitrogen on the surface of a germanium crystal to form hydrated thin films. FTIR spectra were recorded using a ThermoNicolet Nexus 670 FTIR spectrophotometer from 4000 to 400 cm^{-1} using a 4 cm^{-1} resolution and an accumulation of 64 scans. After recording the FTIR spectra of the samples before H/D exchange in triplicate, the exchange was initiated by flushing the hydrated thin films with D_2O-saturated nitrogen. FTIR spectra were then recorded every 2 min for the first 20 min and at different time intervals thereafter for the next 8 h. The intensities of the amide II band were extrapolated from the spectra obtained as a function of exchange. These values were corrected for film swelling by subtracting the intensities at 1305 cm^{-1}, a wavenumber at which the absorbance was independent of the exchange and only affected by film swelling. The ratios of the corrected amide II peak intensities over the corrected initial amide II peak intensity were used to follow the kinetics of exchange.

Circular Dichroism (CD) Measurements. Far-UV CD spectra of LEN solution at pH 2 (20 mM HCl and 100 mM NaCl) and 3 mg/mL were measured as a function of stirring time using a 60DS spectropolarimeter (Aviv, NJ). Protein solutions were stirred at 37 °C and 630 rpm in a 2 mL HPLC glass vial containing a microstirrer bar. Aliquots of 40 μL were withdrawn after 0, 4, 12, and 24 h of stirring and spun for 10 min at 18 000*g* to remove possible insoluble material. However, up to 24 h, no pellets and no significant decrease in the protein content of the supernatants were observed. The protein concentration of the supernatants was measured by UV absorbance at 280 nm using an extinction coefficient ($\epsilon_{1mg/mL}$) of 1.81. Far-UV CD spectra were recorded at a protein concentration of 3 mg/mL from 250 to 200 nm using a circular cell with a 0.01 cm path length. After buffer subtraction, the CD spectra were corrected for protein concentration and smoothed using the Savitsky−Golay function (using a second-order polynomial function with five points).

Acrylamide Quenching. Quenching experiments on LEN solution at pH 2 (20 mM HCl and 100 mM NaCl) were performed as a function of stirring time by following the intrinsic fluorescence intensity of protein solutions upon adding a series of 5 μL aliquots of a 3 M acrylamide solution. Protein solutions were stirred at 37 °C and 660 rpm in a 2 mL HPLC glass vial containing a microstirrer bar. Aliquots of 50 μL were withdrawn after 0, 4, 12, and 80 h of stirring and diluted into 950 mL of a pH 2 dilution solution (20 mM HCl and 100 mM NaCl) to obtain a final protein concentration of 0.15 mg/mL. The fluorescence measurements were performed using a FluoroMax-2 fluorescence spectrophotometer (Jobin Yvon-Spex) with an excitation wavelength of 280 nm (3 nm band-pass) and recording the emission spectra from 300 to 420 nm (3 nm band-pass). Fluorescence intensities were further corrected for dilution because of the stepwise addition of acrylamide. The values of the Stern−Volmer constant (K_{SV}) or dynamic quenching were obtained by curve-fitting the experimental data to the following equation:

$$F_0/F = (1 + K_{SV}[A]) \exp(K_{ST}[A]) \quad (3)$$

where F_o and F are the fluorescence intensities in the absence and presence of acrylamide, respectively, [A] is the concentration of acrylamide, and K_{ST} represents the static quenching constant responsible for a slight upward curvature. Since similar protein/acrylamide ratios were used throughout the experiment, the presence of similar static quenching between acrylamide and LEN was assumed. Thus, the same value of K_{ST} was used for the curve fitting of all data.

Protein Stability toward Urea. The urea stability of LEN solutions at pH 2 (20 mM HCl and 100 mM NaCl) and 3 mg/mL was measured as a function of incubation time. Protein solutions were stirred at 37 °C and 660 rpm in a 2 mL HPLC glass vial containing a microstirrer bar. Aliquots were withdrawn after 0, 4, 12, and 80 h of stirring. Samples were incubated in increasing amounts of urea (from 0 to 9 M) for 4 h at room temperature to ensure complete unfolding equilibrium. The final protein concentration was 0.01 mg/mL. Protein stability was assessed by measuring LEN intrinsic tryptophan fluorescence intensity (for the sample before stirring) or emission maximum (for the samples after 4, 12, and 80 h of stirring). The fluorescence measurements were performed using a FluoroMax-2 fluorescence spectrophotometer (Jobin Yvon-Spex) by exciting the samples at 280 nm (5 nm band-pass) and recording the emission spectra from 300 to 420 nm (5 nm band-pass).

Assuming a two-state folding mechanism, the fraction of the unfolded conformation (F_u) was obtained using the following equation:

$$F_u = (y_f - y)/(y_f - y_u) \quad (4)$$

where y_f and y_u represent the tryptophan fluorescence value of y characteristic of the folded and unfolded conformations, respectively, under the conditions where y is being measured (*13*). The values of y_f and y_u were obtained by linear regression on the data points before and after the unfolding transition, respectively. A sigmoidal curve fit was subsequently used to determine the midpoints of the unfolding transition (C_m).

Limited Pepsin Proteolysis Coupled with Nonreducing SDS−PAGE. The stability of LEN samples toward partial proteolysis was determined as a function of incubation time. Protein solutions were stirred at 37 °C and 660 rpm in a 2 mL HPLC glass vial containing a microstirrer bar. Protein samples after 0, 4, 12, and 80 h of stirring were subjected to proteolysis using pepsin at pH 2 and a weight ratio of 1:100 (enzyme to LEN). Aliquots of the digestion products were withdrawn after 0, 60, 120, 180, and 240 min and assayed on nonreducing SDS−PAGE gels. The digestion process was quenched by adding SDS buffer and boiling the samples for

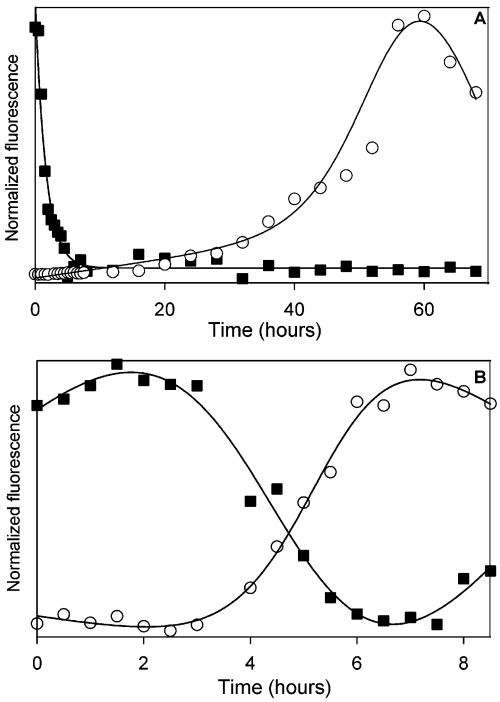

FIGURE 1: (A) ThT (fibril formation, ○) and ANS λ_{max} position (structural reorganization, ■) profiles for LEN solution at 3 mg/mL and pH 2. (B) ThT (fibril formation, ○) and ANS λ_{max} position (structural reorganization, ■) profiles for LEN solution at 0.01 mg/mL and pH 2.

5 min. SDS−PAGE was performed using precast 20% homogeneous acrylamide gels and SDS buffer strips (Phast-Gel, Pharmacia) on an automated separation unit (Phast-System, Pharmacia). Gels were stained using Coomassie blue (Blue R, Pharmacia).

Static Light Scattering. Rayleigh scattering measurements were performed using a FluoroMax-2 fluorescence spectrophotometer (Jobin Yvon-Spex) with excitation and emission at 330 nm and slit widths of 3 nm.

RESULTS

With vigorous agitation, LEN at pH 2 was shown to form fibrils in an inverse concentration-dependent manner, the kinetics becoming slower as the protein concentration was increased (Figure 1) (*9*). Upon stirring LEN solution at high protein concentration (3 mg/mL or 240 μM) and pH 2, the formation of off-pathway soluble oligomers was demonstrated prior to the formation of fibrils, resulting in slow kinetics of fibril formation (*9*). To better characterize these oligomeric species as a function of incubation time, various biophysical techniques were used to monitor structural changes on stirring LEN solutions at 3 mg/mL and pH 2.

Changes in Fluorescence Anisotropy and Light Scattering as a Function of Stirring Time. Steady-state fluorescence anisotropy has been used to compare protein conformation among mutant proteins (*14*) and to follow protein unfolding in guanidine hydrochloride (*15*) and changes in protein structure upon ligand binding (*16*). In this study, steady-state Trp fluorescence anisotropy was used to follow changes occurring in LEN solutions on stirring at pH 2 and 3 mg/mL. A rapid initial increase of the anisotropy values through the first 24 h of stirring, followed by a slower increasing phase during fibril formation, was observed (Figure 2). This

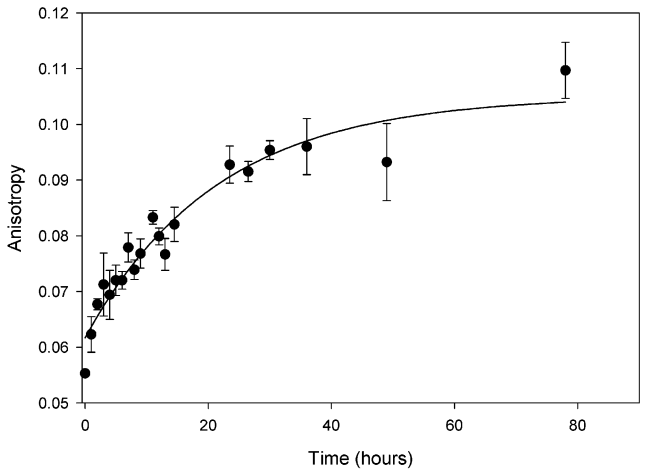

FIGURE 2: Anisotropy measurement of LEN solution at pH 2 (20 mM HCl and 100 mM NaCl) as a function of stirring time. LEN solution was stirred at 3 mg/mL, 37 °C, and 630 rpm. Aliquots of protein solution were withdrawn at predetermined time points, and the anisotropy of the diluted samples was measured using tryptophan fluorescence.

constant increase in anisotropy is attributed to an increase in size of the species in solution. The initial anisotropy value of LEN solution was 0.0553 ± 0.0006. During the first 24 h of stirring, where no fibrils were observed (based on ThT fluorescence assay) (Figure 1), the anisotropy progressively climbed to 0.0928 ± 0.0033, indicating a steady increase in the size of the species in solution. Upon further stirring and the appearance of fibrils, the anisotropy increased more slowly to 0.1097 ± 0.0050 after 80 h, reflecting the increase in size of the species now in suspension as compared to the oligomers previously present in solution.

The early stages of the kinetic experiment (the first 24 h) were also monitored by static light scattering and electron microscopy. A rapid and progressive increase in scattering was observed throughout the first 24 h of stirring (data not shown), confirming a progressive increase in size and/or in numbers of the scattering particles in solution prior to fibril formation. EM images showed clusters of small particles at 3 h and much denser deposits of larger size material at 6−16 h. A few fibrils appeared at 20 h and were quite common by 24 h. Most of the deposited material was fibrils by 60 h.

Changes in Secondary Structure as a Function of Stirring Time. Far-UV CD spectra were recorded after 0, 4, 12, and 24 h of stirring (Figure 3). As previously reported (*9*), the far-UV CD spectra of LEN at pH 2 is unusual because of the contributions of aromatic groups in the 210−230 nm region. The initial CD spectrum (before stirring) was characterized by two minima (at 235 and 219 nm). While the minimum at 219 nm is characteristic of β-structures, the one at 235 nm is attributed to the contributions of aromatic clusters (*17*). After 4 h of stirring, an increase in negative ellipticity at 218 nm was observed simultaneously with the disappearance of the band at 235 nm. These two observations probably reflect the oligomerization of the species in solution with a concomitant disruption of the aromatic clusters. After 12 h of stirring, a further increase in negative ellipticity at 218 nm was observed, indicating additional association. Interestingly, a shoulder at about 205 nm also appeared, attributed to the presence of increased disordered structure in the species present in solution at that stage of the kinetic

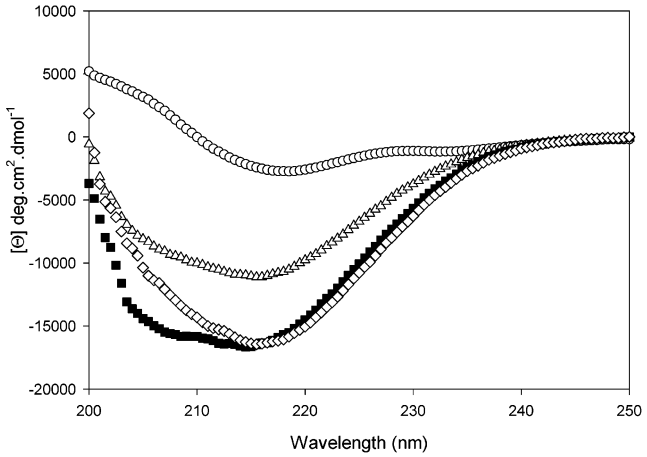

FIGURE 3: Far-UV CD of LEN solution at pH 2 (20 mM HCl and 100 mM NaCl) as a function of stirring time: 0 h (○), 4 h (△), 12 h (■), and 28 h (◇). LEN solutions were stirred at 3 mg/mL, 37 °C, and 630 rpm. The spectra were obtained at a protein concentration of 3 mg/mL using a 0.01 cm path length circular cell.

experiment. After 24 h of stirring, no additional changes in the β-band were observed, but the shoulder at 205 nm had disappeared.

Samples taken after 0, 4, 12, and 80 h of stirring were also studied by hydrated thin film ATR-FTIR. Initially, the peak maximum of the amide I region of LEN at pH 2 was observed at 1638 cm^{-1}, typical for a β-protein. After 4 h of stirring, both a small band broadening and a slight shift of the peak maximum toward lower wavenumbers (1636 cm^{-1}) were detected, reflecting association of the species in solution. However, no dramatic changes were observed after only 4 h of stirring in the secondary derivative spectra, probably indicating the absence of significant structural reorganization. On the other hand, after 12 h of stirring, a significant shift of the peak maximum toward lower wavenumbers (1630 cm^{-1}) was observed simultaneously with a further broadening of the peak. Significant changes in the secondary derivative spectra were also detected. The sizable shift in the peak maximum indicates some reorganization of the β-structure, while the band broadening is ascribed to further association. The sample withdrawn after 80 h, solely composed of fibrils, was characterized by a peak maximum at 1632 cm^{-1}. Again, the secondary derivative spectrum revealed the presence of significant structural rearrangement upon fibril formation. Curve fitting of the amide I regions was performed with the raw spectra (Figure 4) to determine, in more detail, the changes in secondary structure of the species in solution as a function of stirring time (Table 1). The analysis revealed that LEN was initially composed of 68 ± 3% β-sheet, with peaks at 1637 and 1676 cm^{-1}. A peak at 1662 cm^{-1} reflected the presence of turns and loops, corresponding to about 23% of the structure. Very little change was observed after only 4 h of stirring, despite the occurrence of oligomerization (as demonstrated by the different scattering techniques): only a small increase in the peak corresponding to the turns/loops (from about 23 to 30%). After 12 h of stirring, however, changes in both peak position and area were observed, reflecting significant structural reorganization of the species in solution. A shift of the main β-peak from 1637 to 1627 cm^{-1} occurred concomitantly to a decrease in its relative area (from about

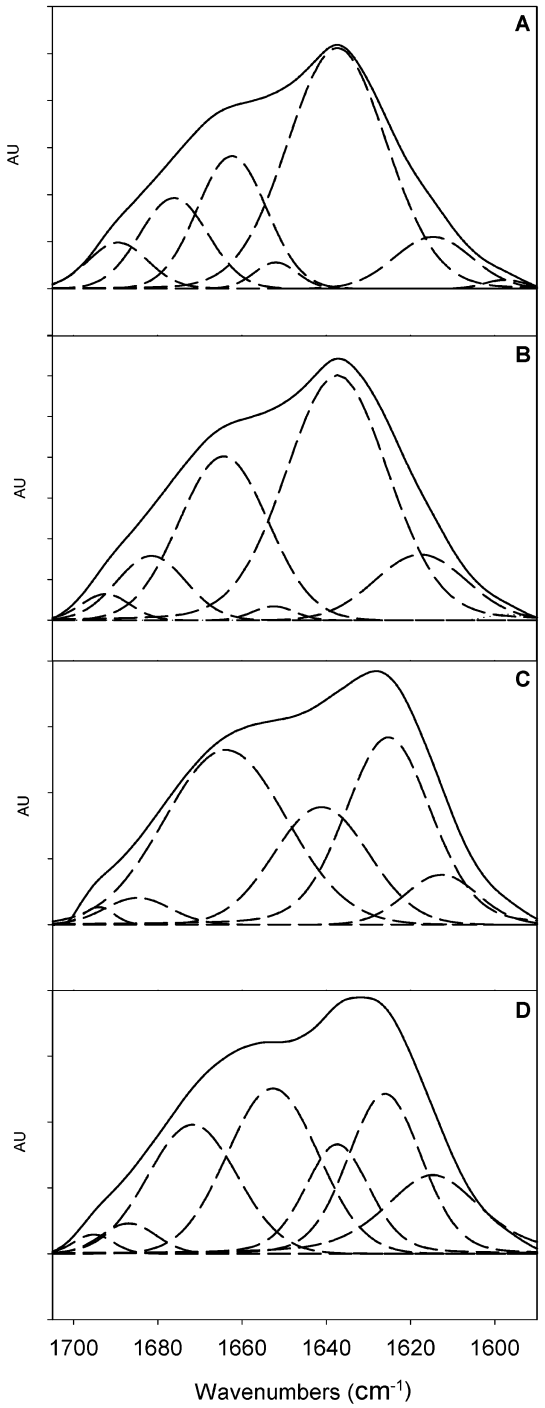

FIGURE 4: Amide I region of the FTIR spectra of LEN solution at pH 2 (20 mM HCl and 100 mM NaCl) as a function of stirring time: 0 h (A), 4 h (B), 12 h (C), and 80 h (D). LEN solutions were stirred at 3 mg/mL, 37 °C, and 630 rpm. The solid lines represent the raw ATR-FTIR spectra after water subtraction. The dotted lines represent the curve-fitted components used for secondary structure analysis.

45 to 33%). Similarly, a shift of the other β-peak to higher wavenumbers (from 1679 to 1685 cm^{-1}), accompanied by a decrease in its area, was detected. Interestingly, a peak at 1641 cm^{-1}, corresponding to unordered structure, was detected concurrently with an increase in the turns/loops peak at 1664 cm^{-1}. (Although the peak at 1641 cm^{-1} could reflect β-sheet/extended structure, we interpret it as unordered structure based on the CD results.) Overall, 56% of the secondary structure content of the species in solution, after

Table 1: Secondary Structure Content of LEN[a]

stirring time (hours)	peak position[b] (cm^{-1})	secondary structure assignment	area under the curve[c] (%)
0	1691	turns	5.5
	1676	β-sheet	20
	1662	turns/loops	23
	1652	α-helix	3
	1637	β-sheet	48.5
4	1691	turns	8.5
	1679	β-sheet	14
	1665	turns/loops	29.5
	1652	α-helix	3
	1637	β-sheet	45
12	1694	turns	4.5
	1685	β-sheet	6.5
	1664	turns/loops	33
	1641	unordered	23
	1625	β-sheet	33
80	1695	turns	3.5
	1686	turns/loops	4.5
	1674	β-sheet	21
	1654	turns/loops	27.5
	1635	β-sheet	17.5
	1626	β-sheet	26

[a] From hydrated thin-film ATR-FTIR spectra at pH 2, 37 °C, 3 mg/mL (240 μM), and various stirring times at 630 rpm. [b] Errors in estimates of peak position were in the order of ±2% ($n = 2$). [c] Errors in estimates of secondary structure content were in the order of ±3% ($n = 2$).

12 h of stirring, corresponded to unordered/loop structures. At the end of the kinetic experiment (after 80 h), the spectrum of the fibrils showed several peaks characteristic of β-sheets (1686, 1674, 1635, and 1627 cm^{-1}), representing about 70% of the secondary structure content.

Changes in Solvent Accessibility and Rate of H/D Exchange as a Function of Stirring Time. Acrylamide quenching has been used to provide insights into conformational changes of proteins by probing the solvent accessibility of fluorescent moieties (*18*−*20*). Quenching experiments were performed on LEN solutions at pH 2 after 0, 4, 12, and 80 h of stirring using the intrinsic Trp fluorescence (Figure 5). The Stern Volmer constants (K_{SV}) obtained from curve fitting the fluorescence data after 0, 4, 12, and 80 h were 6.5 ± 0.1, 3.5 ± 0.1, 4.0 ± 0.1, and 3.2 ± 0.1 M^{-1}, respectively. A significant decrease in the solvent accessibility of the two tryptophan residues was observed after 4 h of stirring, certainly because of the oligomerization process observed immediately upon stirring the protein solution. Interestingly, the solvent accessibility of the tryptophans was slightly higher for the species in solution after 12 h of stirring as compared to those present after only 4 h, despite the ongoing association process (confirmed by several scattering techniques). Upon fibril formation, the solvent accessibility decreased again, as expected for tightly aggregated material. None of the quenching plots were linear (Figure 5); the upward curvatures indicated the presence of static quenching between acrylamide and the fluorophores. This static quenching was taken into account in the equation used for curve-fitting the data (see Materials and Methods).

Determining the rate of hydrogen/deuterium exchange has been used to obtain information on the relative dynamics and accessibility of proteins (*21*−*23*). The rates of H/D exchange using ATR-FTIR were measured on the same protein samples (after 0, 4, 12, and 80 h of stirring). Upon

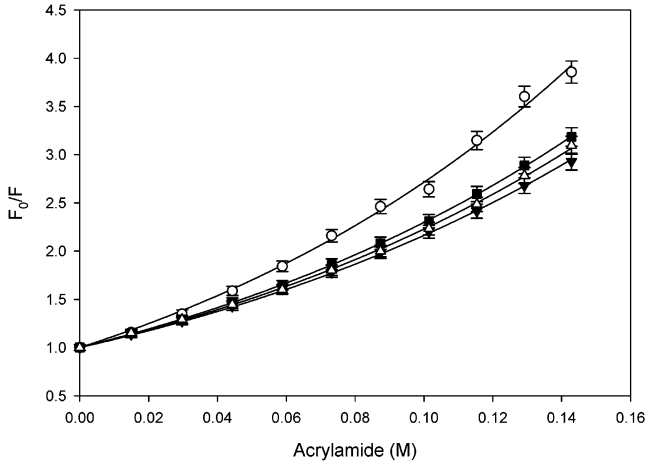

FIGURE 5: Acrylamide tryptophan quenching of LEN solution at pH 2 (20 mM HCl and 100 mM NaCl) as a function of stirring time: 0 h (○), 4 h (△), 12 h (■), and 80 h (▼). LEN solutions were stirred at 3 mg/mL, 37 °C, and 630 rpm. The final protein concentration during the fluorescence measurement was 0.15 mg/mL. The lines represent the best nonlinear curve-fit to determine the Stern−Volmer constants.

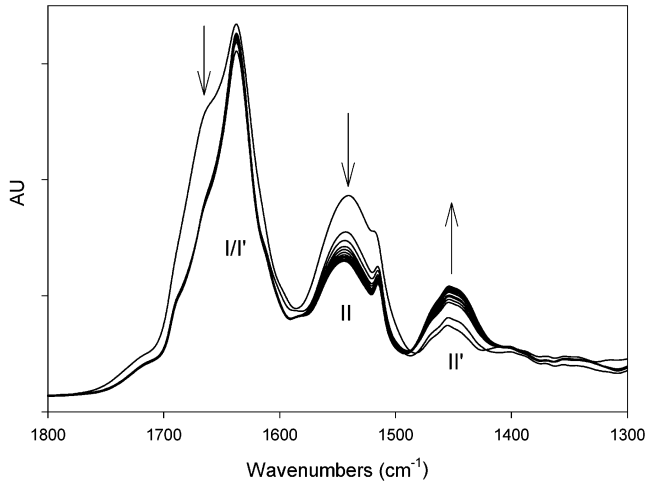

FIGURE 6: Thin film ATR-FTIR spectra of LEN solution at pH 2 (20 mM HCl and 100 mM NaCl) during H/D exchange. 120 μg of protein was dried on a germanium crystal. Deuterium-saturated nitrogen was blown onto the samples, and IR spectra were recorded at predetermined time points during the exchange. The arrows point in the direction of changes in intensity during the exchange.

exchanging the accessible protons, a progressive decrease in the intensities of the amide I and II regions was observed concomitant to an increase in that of the amide II′ region (Figure 6). After correcting for film swelling, the rates of exchange were estimated by taking the ratio of the amide II intensities obtained during exchange over the initial amide II intensity (Figure 7). After 4 h of stirring, a slight decrease in both the rate of exchange and the total amount of exchangeable protons, as compared to those initially measured, was observed. Again, a significant increase in the rate and the total amount of exchanged protons was detected for the samples withdrawn after 12 h of stirring, as compared not only to the 4 h sample but also to the initial one. The rate of H/D exchange of the fibrils was slightly slower than that at the beginning of the incubation, presumably reflecting a small degree of solvent protection in the fibrils. The key feature of the H/D exchange data, however, is that the results

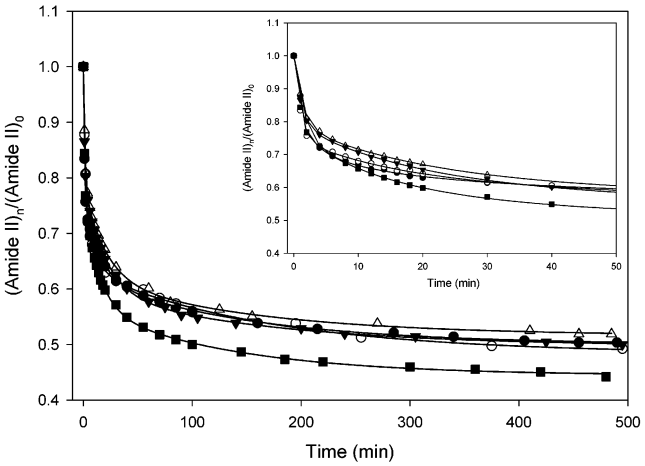

FIGURE 7: H/D exchange kinetics of LEN solution at pH 2 (20 mM HCl and 100 mM NaCl) as a function of stirring time: 0 h (○,●), 4 h (△), 12 h (■), and 80 h (▼). LEN solutions were stirred at 3 mg/mL, 37 °C, and 630 rpm. Aliquots of 40 μL of protein solution (or 120 μg of protein) were dried on a germanium crystal at each time point. IR spectra were recorded during the exchange. After correction for film swelling, the ratios of the amide II peak intensities over the initial amide II peak intensity were used to follow the kinetics of exchange. The insert represents the early time points of exchange. The average standard deviation in the ratios of amide I/II intensities was 1.5−2.0%.

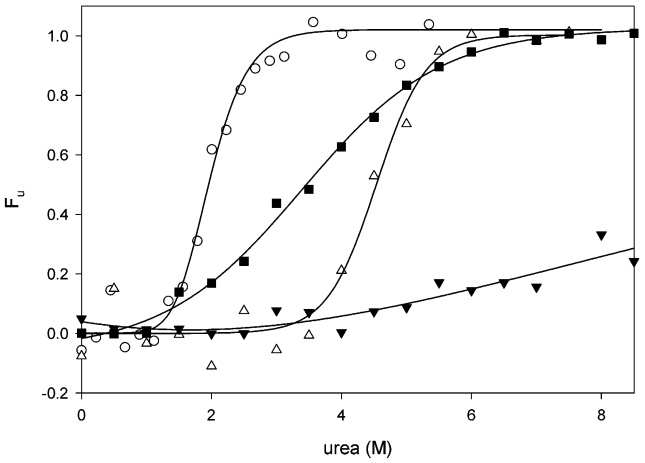

FIGURE 8: Urea stability of LEN solution at pH 2 (20 mM HCl and 100 mM NaCl) as a function of stirring time: 0 h (○), 4 h (△), 12 h (■), and 80 h (▼). LEN solutions were stirred at 3 mg/mL, 37 °C, and 630 rpm. Intrinsic fluorescence intensity was used to monitor the unfolding of LEN before stirring, whereas the peak position maxima were used for the samples after 4, 12, and 80 h of stirring. The final protein concentration during the urea incubation and fluorescence measurement was 0.01 mg/mL. The solid lines represent the best curve fit for the determination of the urea concentrations corresponding to the midpoint of the transitions (C_m).

for 12 h indicate significantly faster and more exchange than under other conditions.

Changes in Urea and Proteolysis Stabilities as a Function of Stirring Time. The urea stability of LEN samples after stirring for 0, 4, 12, and 80 h was studied (Figure 8). As previously reported (*9*), the C_m values for the 0- and 4-h samples were 2.0 ± 0.04 and 4.5 ± 0.1 M, respectively. The increase in stability of the 4-h samples was consistent with the formation of soluble oligomers. After 12 h of stirring, a C_m value of 3.4 ± 0.1 M reflected a decrease in stability. The fibrils (80-h sample) were not significantly

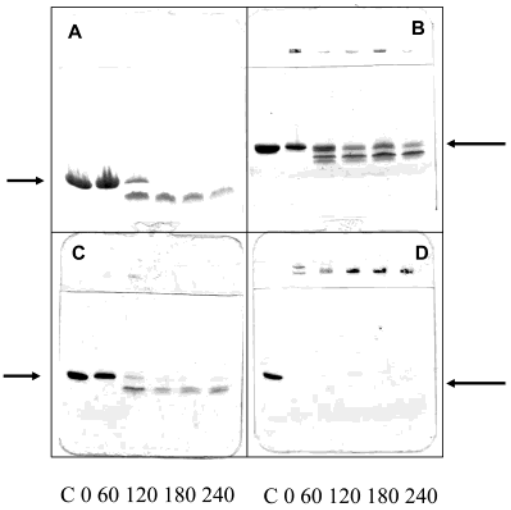

FIGURE 9: SDS−PAGE gels of pepsin digests of LEN solution at pH 2 (20 mM HCl and 100 mM NaCl) as a function of stirring time: 0 h (A), 4 h (B), 12 h (C), and 80 h (D). LEN solutions were stirred at 3 mg/mL, 37 °C, and 630 rpm. Aliquots of protein solution were withdrawn at the indicated time points (0−240 min, C = control − untreated LEN) and incubated with a LEN/pepsin ratio of 100:1. The arrows indicate the position of intact LEN.

unfolded by 8.5 M urea, clearly reflecting the increased stability of such ordered aggregated species.

Limited proteolysis experiments have been used to monitor conformational transition of proteins (*24*−*27*) as well as to obtain insights on amyloid fibril structure (*28*). The stability of the LEN samples stirred for 0, 4, 12, and 80 h toward partial proteolysis was studied. The samples were incubated with pepsin at pH 2. Aliquots of the digestion mixture taken after 0, 60, 120, 180, and 240 min were assayed by SDS−PAGE gels (Figure 9). The disappearance of the LEN band with the concomitant appearance of low molecular weight bands was used to estimate the extent and rate of proteolysis. The digestion of the 0-h sample was complete after 120 min, the intact LEN band not being detected thereafter. In addition, a low molecular band, corresponding to a relatively protease-stable fragment, could be observed (Figure 9A). After 4 h of stirring, a mixture of monomeric LEN and larger species, not entering the separating gel, were observed (lane 2, Figure 9B). This mixture could be the result of solution equilibrium or dissociation of higher oligomers upon boiling in SDS. On incubation with pepsin, the appearance of low molecular weight bands was detected, indicating the proteolysis of LEN monomers by pepsin. However, after 240 min of incubation in the presence of pepsin, a band corresponding to intact LEN was still observed (lane 6, Figure 9B), probably because of dissociation of the nondigested higher oligomers upon boiling the samples in SDS. In any case, the 4-h samples appeared to be more resistant to pepsin proteolysis than native dimers or monomers. After 12 h of stirring, a mixture of monomeric LEN with little higher oligomers was observed, possibly indicating that the oligomers in solution at 12 h were less stable toward boiling SDS than those present in the 4-h sample (lane 2, Figure 9C). On pepsin digestion, low molecular weight bands were observed concomitantly with a decrease in density of the LEN band and the disappearance of the higher oligomeric band in the stacking gel (lanes 3−6, Figure 9C). These observations indicated that the species present after 12 h of stirring were, despite

being somewhat more resistant toward proteolysis than monomeric and dimeric LEN, less stable than the species present in the 4-h sample. After 80 h of stirring, the only protein band detected was in the stacking gel (lane 2, Figure 9D), reflecting both the absence of nonaggregated material in the sample and the high stability of fibrils toward pepsin digestion and boiling SDS.

DISCUSSION

The dissociation constant of LEN at pH 2 was estimated to be 62 ± 20 μM (*9*). In other words, ≈90% of the protein is dimeric at 3 mg/mL (or 240 μM). On stirring solutions of LEN at this concentration, soluble off-pathway oligomeric species were formed prior to the appearance of fibrils, significantly slowing down the kinetics of fibril formation, as compared to those measured at much lower protein concentrations (*9*). However, eventually all the protein in solution was present as fibrils, despite the accumulation of the off-pathway soluble oligomers during the early stages of LEN fibrillation. This observation indicated that some type of structural rearrangements were necessary for the off-pathway soluble oligomers to become fibril-prone. However, such structural reorganization could occur with or without transient dissociation of the oligomeric species. We believe that the results obtained at pH 2 are, in fact, relevant to the physiologic situation, given that the kidneys are the most common site of light chain amyloid deposits. Conditions in the kidneys are significantly destabilizing for proteins. Thus, LEN is likely to significantly populate the conformation present at pH 2; in regions of the kidney, for example, conditions in the distal tubules are pH ~6.5, 50 mM phosphate, 0.1−0.4 M NaCl, and 0.4 M urea, and in the proximal tubules the pH is 4.5, 0.25 M NaCl.

Increase in Size of the Species in Solution. The steady-state fluorescence anisotropy measurements clearly showed a progressive increase in the size of the species in solution throughout the kinetic experiment (Figure 2). Furthermore, no transient decrease in the anisotropy values was observed during the experiment, especially during the first 24 h of stirring. This absence of a decrease in the anisotropy indicates that the oligomeric off-pathway species do not undergo significant dissociation while rearranging into fibril-prone species. A constant increase in Rayleigh scattering values (data not shown) was also observed upon stirring LEN solutions at pH 2. These data are consistent with a continuous increase in size of the species in solution in the early stages of stirring, although the increase in Rayleigh scattering values might not allow differentiation between an increase in size of the scatterers from an increase in the number of scatterers of eventually smaller size. Furthermore, small-angle X-ray scattering was also used to monitor the size of the species present during the early stages of stirring LEN solution at pH 2 and 3 mg/mL (*9*). Forward scattering values $I(0)$, which are proportional to the size of the species in solution at a given concentration, were extrapolated from scattering profiles. A consistent increase in $I(0)$ was observed from the beginning of the kinetic experiment, indicating the formation of soluble species of progressively larger size. These results suggest that the necessary structural reorganization from the off-pathway soluble oligomers to fibril-prone species did not involve major dissociation but was instead occurring while additional association was happening. Thus, to understand this putative reorganization step, secondary structure probes such as far-UV CD and FTIR were subsequently used.

Transient Appearance of Unordered Structures. Despite a continuous increase in size of the species in solution during the transition step from the off-pathway species to fibril-prone entities, both far-UV CD and ATR-FTIR spectra revealed the presence of larger amounts of unordered structure in the 12-h samples than were detected in either the 4-, 24-h sample, or the fibrils (80-h sample). Whereas a broad β-peak was detected after 4 h of stirring, the presence of a marked shoulder at 205 nm was observed on the CD spectrum of the 12-h sample (Figure 3). This shoulder clearly indicated the presence of significant amounts of disordered structure. Interestingly, the shoulder was no longer present in the spectrum of the 24-h sample, indicating the more ordered character of the species in solution just before the first fibrils were formed. Unfortunately, upon fibril formation, CD measurements were no longer possible because of the precipitation of fibrils.

With ATR-FTIR it is possible to examine the secondary structure of not only native proteins in solution but also unfolded and aggregated proteins (*29*, *30*). Despite a small band broadening, probably reflecting association, no significant structural reorganization occurred during the first 4 h of stirring, as indicated by very similar secondary structure content between the 0- and the 4-h samples (Table 1). The increased amount of unordered structure in the 12-h samples was demonstrated by the presence of a peak at 1641 cm^{-1}. Together with the peak at 1664 cm^{-1}, characteristic of loop/turn-type structure, about 56% of the secondary structure content appeared to be somewhat unordered. Again, both the disappearance of the band at 1641 cm^{-1} and the appearance of several bands characteristics of β-structures (probably intra- and intermolecular β-sheets) indicated the structured character of fibrils (Figure 4). The transient appearance of an increased amount of unordered structures is ascribed to the structural reorganization allowing the transformation of the soluble off-pathway oligomers into fibril-prone soluble species. To confirm the interpretation of these results, techniques monitoring the compactness of proteins were used.

Transient Appearance of Less Compact Structures. Acrylamide fluorescence quenching and H/D exchange were used to study the changes in compactness of the various species in solution formed on stirring 3 mg/mL LEN solutions at pH 2. The intrinsic fluorescence of LEN results from two tryptophan residues, at positions 35 and 50. On the basis of the crystal structure of LEN (*31*), one of the tryptophan residues (Trp50) is significantly solvent exposed, whereas the other one (Trp35) is both buried in the hydrophobic core of the protein and quenched by the spatial proximity of the disulfide bridge Cys23−Cys94. Acrylamide fluorescence quenching is a technique that monitors the compactness of proteins by measuring the solvent accessibility of (buried) fluorescent residues, making this technique much more sensitive to the degree of association than techniques such as H/D exchange, which monitors the compactness of proteins by measuring the increased solvent accessibility of exchangeable protons. As expected, on oligomerization immediately after the stirring started, a substantial decrease in the Stern−Volmer constant was detected (Figure 5). This

result indicates that a decrease in solvent accessibility of the fluorophores occurred in the soluble off-pathway oligomers. After 12 h of stirring, an increase in the dynamic quenching was detected, reflecting somewhat greater Trp accessibility, despite the continual increase in size. The possibility of the partial dissociation, occurring at this stage of the aggregation process, appeared to be unlikely based on the scattering data, which clearly shows a continuous increase in size of the species in solution from the beginning of the stirring period. Also, several of the probes (e.g., FTIR, H/D exchange) show unique properties for the species at 12 h, indicating that the sample at that time is not a mixture of earlier and later species. The relatively small amplitude change in the dynamic quenching values between the 4- and the 12-h samples as compared to the much larger difference in the unordered structure content (obtained from the IR data) could simply be explained by the differences between the conformation of an individual molecule, as measured by FTIR, and the overall size of the oligomer, as determined by the acrylamide quenching. In this case, the increase in size of the species in solution and the simultaneous decrease in compactness have opposite effects on the Stern−Volmer constant. As more association occurs, the two tryptophan residues became less and less solvent accessible, irrespective of the overall compactness of the individual molecules. Formation of fibrils led to a further decrease in Trp accessibility, probably reflecting both their increased compactness and their size.

Similar results were detected with H/D exchange. A slower rate of exchange and a decrease in the number of exchangeable protons, as compared to the initial sample, were observed after 4 h of stirring, certainly because of the oligomerization of the dimers initially present. The species present in solution after 12 h of stirring were characterized by a faster rate of exchange and the presence of significantly more proton accessibility, confirming the greater solvent accessibility in the species at 12 h. This increased solvent accessibility is most likely because of a decrease in compactness, which would also be consistent with the acrylamide quenching data (Figure 7). This observation seems to correlate with the significant amount of unordered secondary structure present at 12 h. Surprisingly, the rate of exchange and the number of exchangeable protons for the fibrils (80-h sample) were similar to those of the dimers initially present. This could be explained by the presence of significant amounts of loops and turns on the periphery of the fibril core. In fact, about 28% of the secondary structure content of the fibrils was composed of loops and turns, based on the amide I analysis. Furthermore, based on the significantly lower acrylamide dynamic quenching value obtained for the fibrils as compared to the LEN dimers, it is more likely that neither of the two tryptophan residues were present in these loops but were, instead, buried inside the fibril core. Thus, the results from the probes of secondary structure and compactness suggest a structural rearrangement occurring after about 12 h of stirring.

Transient Decrease in Intrinsic and Proteolysis Stability. Significant changes in urea stability were measured during the incubation of LEN (Figure 8). Particularly noteworthy is that after an initial increase in stability because of formation of the soluble oligomers, a significant decrease in stability was subsequently detected with the 12-h sample. Furthermore, the transition was much less cooperative than those detected for the earlier time points. This could reflect heterogeneity in the size of the oligomers, with the larger ones being more stable than the smaller ones. Once again, this decrease in stability was only transient, the fibrils being very resistant to urea unfolding.

Partial pepsin proteolysis confirmed the changes observed in urea stability. The least protease-susceptible soluble species was that at 4 h of incubation. Interestingly, the 12-h sample was only marginally more resistant than the native dimer. The relative protease-resistance of the 4-h sample probably reflects the fact that essentially all the protein is tied up in large oligomers, in which most of the LEN molecules are inaccessible to the protease and that the conformation is fairly nativelike. The fibrillar material seemed to be completely resistant to proteolysis.

Models for LEN Fibrillation. Normally, the rate of protein aggregation is directly proportional to protein concentration. The inverse protein concentration-dependence on the rate of fibril formation for LEN is thus very unusual. Interestingly, however, fibrils were still observed eventually at high protein concentration, despite the initial trapping of most of the protein as soluble off-pathway oligomers. The key kinetic events in the aggregation of LEN (at pH 2, 3 mg/mL) are as follows: during the first 3 h a soluble oligomer, probably an octamer (*9*), is formed from the dimer. We will call this species I_8. The conformation of the individual molecules in this oligomer correspond to those of the initially formed partially folded intermediate, I, and is relatively nativelike. With time I_8 increases in size, and the component molecules undergo a conformational change leading to a less ordered structure, which we will call $(I^*_8)_n$, whose concentration reaches a maximum around 8−10 h. Then, starting around 20 h, exponential growth of fibrils occurs. In contrast to I, the conformation of I* is much more disordered, as detected by probes of secondary structure, increased susceptibility to proteolysis, increased H/D exchange, and decreased stability. The self-association of the $(I)_8$ oligomers appears to be responsible for the conformational change from I to I*, although a slow time-dependent conformational change of I to I* cannot be ruled out. There is precedent that association of proteins can lead to a conformational change; hence, the structural reorganization occurring from the initial soluble octamers of LEN to the $(I^*_8)_n$ species is attributed to some aspect of the interaction of the octamers, which leads to a more unfolded conformation in the higher oligomers, accounting for the observed decrease in stability and increase in solvent accessibility.

There are two important experimental observations with respect to elucidating the fibrillation pathway. First, a continuous and progressive increase in size from the initial dimers to the fibrils was observed. Second, after the initial formation of soluble oligomers with relatively nativelike conformation (I), a structural reorganization occurred leading to a significantly less structured conformation (I*). These observations suggest two most likely models for the kinetics pathway of fibril formation.

In the first model, Scheme 1, dimers and monomers of LEN undergo a transition to a nativelike partially folded intermediate, I, that rapidly associates to form soluble oligomers, apparently octamers (*9*). These oligomers then undergo a transformation into a second class of soluble

Scheme 1

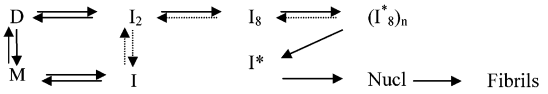

Scheme 2

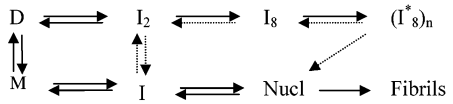

oligomers $(I^*_8)_n$, composed of non-native-like conformations, and that can dissociate to yield monomers of non-native-like conformation (I*). We postulate that these monomeric intermediates, I*, then form the fibril nucleus and go on to form fibrils. Thus, in this model, the soluble oligomeric species $(I^*_8)_n$ acts as a reservoir, effectively making the concentration of monomeric species of LEN very low but slowly releasing fibrillation-prone monomeric species to form fibrils. The appeal of this model is that not only is it consistent with the data, but fibrils are formed from a relatively non-native intermediate, analogous to the case for the closely related amyloidogenic light chain variable domain SMA (*32*).

In the second model, Scheme 2, the $(I^*_8)_n$ species actually acts as the fibrillar precursor, and the fibrils are formed from it through conformational rearrangements. For this model, it is not clear if there is a critical size of oligomer that leads to fibrillation and also whether further changes in conformation of the subunits are required. It is also possible that the I* species shown in Scheme 2 is oligomeric.

For both models, the partially folded intermediate that leads to fibrils is relatively unfolded; thus, the conformational change of LEN in the $(I^*_8)_n$ species is critical for subsequent fibrillation. As noted, this is analogous to the case with SMA (*32*). From the thermodynamic point of view, the second scheme appears more likely.

REFERENCES

1. Harper, J. D., Wong, S. S., Lieber, C. M., and Lansbury, P. T., Jr. (1999) Assembly of Aβ amyloid protofibrils: an in vitro model for a possible early event in Alzheimer's disease, *Biochemistry 38*, 8972−8980.
2. Uversky, V. N., Li, J., and Fink, A. L. (2001) Evidence for a partially folded intermediate in α-synuclein fibril formation, *J. Biol. Chem. 276*, 10737−10744.
3. Khurana, R., Gillespie, J. R., Talapatra, A., Minert, L. J., Ionescu-Zanetti, C., Millett, I. S., and Fink, A. L. (2001) Partially folded intermediates as critical precursors of light chain amyloid fibrils and amorphous aggregates, *Biochemistry 40*, 3525−3535.
4. Jiang, X., Smith, C. S., Petrassi, H. M., Hammarström, P., White, J. T., Sacchettini, J. C., and Kelly, J. W. (2001) An engineered transthyretin monomer that is nonamyloidogenic, unless it is partially denatured, *Biochemistry 40*, 11442−11452.
5. Solomon, A. (1985) Light chains of human immunoglobulin, in *Methods in Enzymology* (Di Sabato, G., Langone, J. J., Van Vunakis, H., Eds.) pp 101−121. Academic Press, San Diego, 116.
6. Solomon, A. Clinical implications of monoclonal light chains (1986) *Semin. Oncology 13*, 341−349.
7. Buxbaum, J. (1992) Mechanisms of disease; monoclonal immunoglobulin deposition. Amyloidosis, light chain deposition disease, and light chain and heavy chain deposition disease, *Hematology-Oncology Clinics of North America 6*, 323−346.
8. Wilkins Stevens, P., Raffen, R., Hanson, D. K., Deng, Y. L., Berrios-Hammond, M., Westholm, F. A., Murphy, C., Eulitz, M., Wetzel, R., Solomon, A., Schiffer, M., and Stevens, F. J. (1995) Recombinant immunoglobulin variable domains generated from synthetic genes provide a system for in vitro characterization of light-chain amyloid proteins, *Protein Sci. 4*, 421−432.
9. Souillac, P. O., Uversky, V. N., Millett, I. S., Khurana, R., Doniach, S., and Fink, A. L. (2002) Elucidation of the molecular mechanism during the early events in immunoglobulin light chain amyloid fibrillation: Evidence for an off-pathway oligomer, *J. Biol. Chem. 277*, 12666−12679.
10. Souillac, P. O., Uversky, V. N., Millett, I. S., Khurana, R., Doniach, S., and Fink, A. L. (2002) Effect of association state and conformational stability on the kinetics of immunoglobulin light chain amyloid fibril formation at physiological pH, *J. Biol. Chem. 277*, 12657−12665.
11. Kolmar, H., Frisch, C., Kleemann, G., Gotze, K., Stevens, F. J., and Fritz, H. J. (1994) Dimerization of Bence Jones proteins; linking the rate of transcription from an *Escherichia coli* promoter to the association constant of REIv, *Biol. Chem. Hoppe-Seyler 375*, 61−70.
12. Nielsen, L., Khurana, R., Coats, A., Frokjaer, S., Brange, J., Vyas, S., Uversky, V. N., and Fink, A. L. (2001) Effect of environmental factors on the kinetics of insulin fibril formation: elucidation of the molecular mechanism, *Biochemistry 40*, 6036−6046.
13. Pace, C. N., Shirley, B. A., and Thomson, J. A. (1996) Chapter 13: Measuring the conformational stability of a protein, in *Protein Structure: A Practical Approach* (Creighton, T. E., Ed.) IRL Press, Oxford.
14. Pittman, I., IV, Nakagawa, S. H., Tager, H. S., and Steiner, D. F. (1997) Maintenance of the B-chain β-turn in [Gly^{B24}]insulin mutants: a steady-state fluorescence anisotropy study, *Biochemistry 36*, 3430−3437.
15. Swaminathan, R., Nath, U., Udgaonkar, J. B., Periasamy, N., and Krishnamoorthy, G. (1996) Motional dynamics of a buried tryptophan reveals the presence of partially structured forms during denaturation of Barstar, *Biochemistry 35*, 9150−9157.
16. Sytnik, A. I., Chumachenko, Y. V., and Demchenko, A. P. (1991) Spectroscopic evidence for NADH-induced conformational changes in rabbit muscle aldolase, *Biochim. Biophys. Acta 1079*, 123−127.
17. Sreerama, N., Manning, M. C., Powers, M. E., Zhang, J. X., Goldenberg, D. P., and Woody, R. W. (1999) Tyrosine, phenylalanine, and disulfide contributions to the circular dichroism of proteins: circular dichroism spectra of wild-type and mutant bovine pancreatic trypsin inhibitor, *Biochemistry 38*, 10814−10822.
18. Eftink, M. R., and Selvidge, L. A. (1982) Fluorescence quenching of liver alcohol dehydrogenase by acrylamide, *Biochemistry 21*, 117−125.
19. Middaugh, C. R., and Litman, G. W. (1978) Investigations of the molecular basis for the temperature-dependent insolubility of cryoglobulins. VI. Quenching by acrylamide of the intrinsic tryptophan fluorescence of cryoglobulin and noncryoglobulin I_gM proteins, *Biochim. Biophys. Acta 535*, 33−43.
20. France, R. M., and Grossman, S. H. (2000) Acrylamide quenching of *apo*- and *holo*-α-lactalbumin in guanidine hydrochloride, *Biochem. Biophys. Res. Commun. 269*, 709−712.
21. De Jongh, H. H. J., Goormaghtigh, E., and Ruysschaert, J. M. (1997) Monitoring structural stability of trypsin inhibitor at the submolecular level by amide-proton exchange using Fourier transform infrared spectroscopy: a test case for more general application, *Biochemistry 36*, 13593−13602.
22. De Jongh, H. H. J., Goormaghtigh, E., and Ruysschaert, J. M. (1997) Amide-proton exchange of water-soluble proteins of different structural classes studied at the submolecular level by infrared spectroscopy, *Biochemistry 36*, 13603−13610.
23. Raschke, T. M., and Marqusee, S. (1998) Hydrogen exchange studies of protein structure, *Curr. Opin. Biotechnol. 9*, 80−86.
24. Fontana, A., Zambonin, M., De Laureto, P. P., De Filippis, V., Clementi, A., and Scaramella, E. (1997) Probing the conformation state of apomyoglobin by limited proteolysis, *J. Mol. Biol. 266*, 223−230.
25. Hubbard, S. J. (1998) The structural aspects of limited proteolysis of native proteins, *Biochim. Biophys. Acta 1382*, 191−206.
26. De Laureto, P. P., Scaramella, E., Frigo, M., Wondrich, F. G., De Filippis, V., Zambonin, M., and Fontana, A. (1999) *Protein Sci. 8*, 2290−2303.
27. Spolaore, B., Bermejo, R., Zambonin, M., and Fontana, A. (2001) Protein interactions leading to conformational changes monitored by limited proteolysis: Apo form and fragments of horse cytochrome *c*, *Biochemistry 40*, 9460−9468.

28. Kheterpal, I., Williams, A., Murphy, C., Bledsoe, B., and Wetzel, R. (2001) Structural features of the Aβ amyloid fibril elucidated by limited proteolysis, *Biochemistry 40*, 11757−11767.
29. Oberg, K. A., and Fink, A. L. (1998) A new attenuated total reflectance Fourier transform infrared spectroscopy method for the study of proteins in solution, *Anal. Biochem. 256*, 2−106.
30. Fink, A. L., Seshadri, S., and Khurana, R. (1999) Attenuated total reflectance FTIR of aggregated proteins, *Methods Enzymol. 309*, 559−576.
31. Huang, D. B., Chang, C. H., Ainsworth, C., Johnson, G., Solomon, A., Stevens, F. J., and Schiffer, M. (1997) Variable domain structure of κIV human light chain LEN: high homology to the murine light chain McPC603, *Mol. Immunol. 34*, 1291−1301.
32. Khurana, R., Gillespie, J. R., Talapatra, A., Minert, L. J., Ionescu-Zanetti, C., Millett, I., and Fink, A. L. (2001) *Biochemistry 40*, 3525−3535.

BI034652M